Structural properties of the two-dimensional triangular antiferromagnet $NiGa_2S_4$

Yusuke Nambu,[1] Robin T. Macaluso,[2] Tomoya Higo,[1] Kenji Ishida,[3] and Satoru Nakatsuji[1]
[1]*Institute for Solid State Physics, University of Tokyo, Kashiwa, Chiba 277-8581, Japan*
[2]*School of Chemistry and Biochemistry, University of Northern Colorado, Greeley, Colorado 80639, USA*
[3]*Department of Physics, Kyoto University, Kyoto 606-8502, Japan*
(Received 6 December 2008; revised manuscript received 23 April 2009; published 12 June 2009)

Polycrystalline samples of $NiGa_2S_{4+\delta}$ ($-0.2 \leq \delta \leq +0.2$) have been synthesized by solid-state reaction. X-ray powder-diffraction measurements indicate that these samples are single phase with a trigonal lattice with a nominal concentration δ at least between −0.12 and +0.16. Rietveld analyses for time-of-flight neutron-diffraction data have revealed that there is no site mixing between Ni and Ga atoms, indicating that the triangular lattice is only formed by Ni atoms. Our susceptibility measurements have clarified that the freezing temperature and the magnitude of hysteresis systematically change with nominal sulfur concentration and form a respective peak and minimum at the nominal $NiGa_2S_{4.04}$. These results together with our chemical analyses indicate that the actual content of sulfur for the nominal $NiGa_2S_{4.04}$ should be stoichiometric, namely, 4.00. On the contrary, the Ga nuclear quadrupole resonance (NQR) has suggested the presence of two different Ga sites from the Ga-NQR spectra in both samples with the nominal concentration of $NiGa_2S_{4.00}$ and $NiGa_2S_{4.04}$, despite the fact that there is a single crystallographic site for Ga in the unit cell. High-resolution transmission electron microscopy scans conducted over a wide region of a $NiGa_2S_{4.04}$ single crystal found a clean defect-free in-plane structure. Diffraction patterns of the selected area indicate the partial presence of a superlatticelike stacking fault. This suggests that the two different Ga sites are not generated by the sulfur deficiency but by the superlatticelike stacking fault.

DOI: 10.1103/PhysRevB.79.214108 PACS number(s): 61.72.Nn, 68.37.Lp, 75.40.Cx, 75.50.Ee

I. INTRODUCTION

Spin systems with low dimensionality and geometrical frustration have attracted a lot of interest in condensed-matter physics because of the potential emergence of novel phenomena upon suppression of conventional magnetic orders.[1] The two-dimensional (2D) triangular lattice antiferromagnets (AFMs) have been intensively studied as one of the simplest form of the geometrical frustrated magnets. Experimentally, however, most triangular lattice AFMs exhibit magnetic long-range ordering because of the coupling between the triangular lattice layers.

The inorganic compound $NiGa_2S_4$ (Refs. 2 and 3) is an example of bulk low spin ($S=1$) 2D AFM with an exact triangular lattice. $NiGa_2S_4$ consists of a NiS_2 layer separated between two GaS layers by a van der Waals gap. The Ni atoms in the NiS_2 layer are arranged in a triangular lattice plane. Interestingly, this compound does not form a conventional three-dimensional (3D) antiferromagnetic (AF) order at least down to 0.08 K despite the fact that its AF interaction has the energy scale of about 80 K. Instead, ^{69,71}Ga nuclear magnetic/quadrupole resonance (NMR/NQR) (Ref. 4) and muon spin-relaxation (μSR) (Ref. 5) experiments have clarified unusual bulk spin freezing across $T^*=8.5$ K that has a highly extended critical regime down to 2 K. Below 2 K, neutron measurements have revealed a quasi-2D (quasi-two-dimensional) noncollinear correlation whose spin-spin in-plane correlation length stays finite around seven times the lattice spacing, while the interplane correlation is so weak that it barely reaches the nearest-neighbor planes.[6] Moreover, inhomogeneous internal field at the Ga site was observed, and the nuclear spin-lattice relaxation rate shows nearly cubic temperature dependence below 1 K that suggests a 2D magnonlike dispersive mode. Further consistent results have been obtained for the magnetic specific heat (C_M) that shows the quadratic temperature dependence below about 4 K, suggesting an AF spin-wave-like mode in 2D despite the absence of a long-range AF order.

Our recent study of the impurity-substituted systems of $Ni_{1-x}A_xGa_2S_4$ (A=Mn, Fe, Co, and Zn) (Ref. 7) as well as the isostructural compound $FeGa_2S_4$ (Ref. 8) has clarified a distinct spin dependence of the low-temperature magnetic properties.[9,10] With nonmagnetic Zn^{2+} and Heisenberg Fe^{2+} ($S=2$) substitution, this quadratic temperature-dependent specific heat is found to be robust and there is no conventional spin-glass behavior featured by $C_M \sim T$ even with a sizable amount of the substitution. In addition, the scaling of $C_M(T)$ with the Weiss temperature (θ_W) strongly provides another evidence for the existence of the 2D AF magnonlike mode, given the fact that θ_W is determined by in-plane interactions not by an interplane coupling. On the other hand, the substitution of Mn^{2+} ($S=\frac{5}{2}$) with a Heisenberg type spin and Co^{2+} ($S=\frac{3}{2}$) with an Ising-type anisotropy induces a conventional spin-glass-like phase at low temperatures. These indicate that the unusual spin state of $NiGa_2S_4$ is not a conventional spin glass, and its 2D AF spin-wave-like behavior represented by $C_M \sim (T/|\theta_W|)^2$ appears only for integer Heisenberg spins.[10] Furthermore, the distinct behaviors between integer and half-integer-substituted spins suggest a quantum effect inherent at low temperatures. Thus, $NiGa_2S_4$ displays an interesting low-temperature spin state associated with 2D frustration.

Although there exists only one crystallographic site for Ga in $NiGa_2S_4$, two distinct Ga signals were found by NMR and NQR measurements even in high-quality powder samples.[4] The origin of the two Ga sites with a slightly different electric field gradient (EFG) at the Ga nuclear site is an important issue to be clarified. It has not been fully un-

derstood, but there are several possibilities, which include sulfur deficiency in the outer sulfur layers and site mixing between Ni and Ga. It is broadly recognized that the systems with geometrical frustration are quite sensitive to impurities and/or randomness. In fact, for NiS_{2+x},[11] the antiferromagnetic transition and the magnetic moment for the weak ferromagnetism sensitively depend on stoichiometry. Another possibility of the origin of the two Ga-NQR signals is that the possible inclusion of a similar compound with slightly different stacking sequence along the c axis induces a stacking fault along the c axis since the layered $NiGa_2S_4$ has the strong two dimensionality due to a van der Waals gap. In a similar structure $ZnIn_2S_4$, for example, there are polytypic structures with $Z=1$, 2, and 3,[12–15] where Z is the number of formula unit in a crystallographic unit cell.

Here we report the detailed study of the structural properties of $NiGa_2S_4$. Our susceptibility measurements using the polycrystalline samples of $NiGa_2S_{4+\delta}$ $(-0.12 \leq \delta \leq +0.16)$ have clarified that the freezing temperature and the magnitude of hysteresis systematically change with the nominal sulfur concentration and form a respective peak and minimum at the nominal $NiGa_2S_{4.04}$. These susceptibility results for $NiGa_2S_{4+\delta}$ with different sulfur content δ as well as our chemical analyses suggest that the sulfur content is actually stoichiometric at the nominal $NiGa_2S_{4.04}$. Rietveld analyses for time-of-flight neutron diffraction were performed to investigate the occupancy and site mixing between Ni and Ga. The results indicate that the occupancy fractions of Ni and Ga refined to values of 1, and that there is no site mixing between the two sites. Furthermore, high-resolution transmission electron microscopy (TEM) observations have been performed to check local structures. Although most of the diffraction pattern of $NiGa_2S_{4.04}$ indicates a clean defect-free in-plane structure of $NiGa_2S_4$, some of the diffraction peaks along the c axis are split. TEM results indicate that $NiGa_2S_{4.04}$ has a nearly perfect triangular lattice formed in the NiS_2 layer for the in-plane structure but also superlatticelike stacking faults for the interlayer structure. In addition, the NQR measurement found two Ga-NQR signals for each isotope even in $NiGa_2S_{4.04}$ as in $NiGa_2S_{4.00}$. Because in $NiGa_2S_{4.04}$ both sulfur deficiency and site mixing are absent, the superlatticelike stacking fault is most likely the origin for the two different NQR peaks in the Ga-NQR spectra.

II. EXPERIMENTAL

Polycrystalline samples with a starting nominal formula of $NiGa_2S_{4+\delta}$ are synthesized by annealing the mixture of elements (4N nickel, 5N gallium, and 4N sulfur) at 900 °C in evacuated quartz ampoules. Prior to the annealing at 900 °C, a preannealing at 400 °C was performed to prevent an explosion due to vaporization of sulfur. After the initial annealing for 5 days, the samples were homogenized by grinding, resealed, and annealed again for 4 days at 900 °C. All the samples described in this paper were synthesized by the same annealing sequences.

Single crystals were prepared by using a chemical vapor transport method in evacuated quartz ampoules. Polycrystalline samples with appropriate nominal concentration, which will be discussed later, were used as starting materials for the crystal growth. The transport reactions were carried out in a temperature gradient 925–850 °C using iodine as a transport agent with the concentration of 3 mg/cm^3.

Structural studies of powdered samples of both polycrystalline and single crystalline samples were performed by x-ray powder diffraction (XRD) at room temperature. The measurements were carried out with Cu Kα ($\lambda = 154.056$ pm) radiation.

Time-of-flight neutron-diffraction data were collected at Argonne National Laboratory's Intense Pulsed Neutron Source-Special Environment Powder Diffractometer on a powder sample at room temperature.[16] The data sets were analyzed using the GSAS/EXPGUI program suite.[17,18] Samples were placed in vanadium cans and diffraction peaks from vanadium were refined as a second phase in the analysis. Background, profile, extinction, absorption, and zero coefficients together with structural parameters and occupancies were refined in the fitting procedure.

dc magnetization M was measured between $T=1.8$ and 350 K under magnetic field up to $\mu_0 H=7$ T using a commercial superconducting quantum interference device magnetometer (Magnetic Properties Measurement System, Quantum Design).

Scanning electron microscopy energy dispersive x-ray (SEM-EDX) measurements were taken on an instrument (JSM-5600, JEOL). The accelerating voltage was 15 kV with beam to sample distance of 20 mm. Approximately eight scans on a crystal with dimensions of 10×10 μm^2 were performed.

The NQR measurements were performed in polycrystalline samples on two Ga isotopes [^{69}Ga ($I=\frac{3}{2}$): $^{69}\gamma = 10.219$ MHz/T and $^{69}Q=0.19\times10^{-24}$ cm^2, ^{71}Ga ($I=\frac{3}{2}$): $^{71}\gamma=12.984$ MHz/T and $^{71}Q=0.16\times10^{-24}$ cm^2, where γ and Q are the gyromagnetic ratio and the electric quadrupole moment, respectively]. The nuclear spin-spin relaxation rate $1/T_2$ was measured by recording the spin-echo intensity $I(2\tau)$ as a function of the time separation τ between the $\pi/2$ (first) and π (second) pulses.[4] $I(2\tau)$ can be well fitted by the relation of $I(2\tau) \propto \exp(-2\tau/T_2)$. The Ga-NQR spectra were obtained by measuring the spin-echo intensity as a function of frequency after T_2 correction.

Transmission electron microscopy observations were carried out using an instrument (JEM-2010F, JEOL) operating at 200 kV. Image simulations were performed with the MACTEMPAS software.[19]

III. RESULTS AND DISCUSSION

Room-temperature XRD analyses for polycrystalline samples with nominal δ between −0.12 and +0.16 indicate that samples are single phase and crystallize in the space group $P\bar{3}m1$. The syntheses with starting compositions of $NiGa_2S_{3.80}$ and $NiGa_2S_{4.20}$ did not form single phases but also contained impurity phases including NiS_2 and Ga_2S_3.

The Rietveld analyses for time-of-flight neutron-diffraction data of $NiGa_2S_4$ (Fig. 1) showed that Ni and Ga fully occupy the 1b and 2d sites, respectively. Fitting results

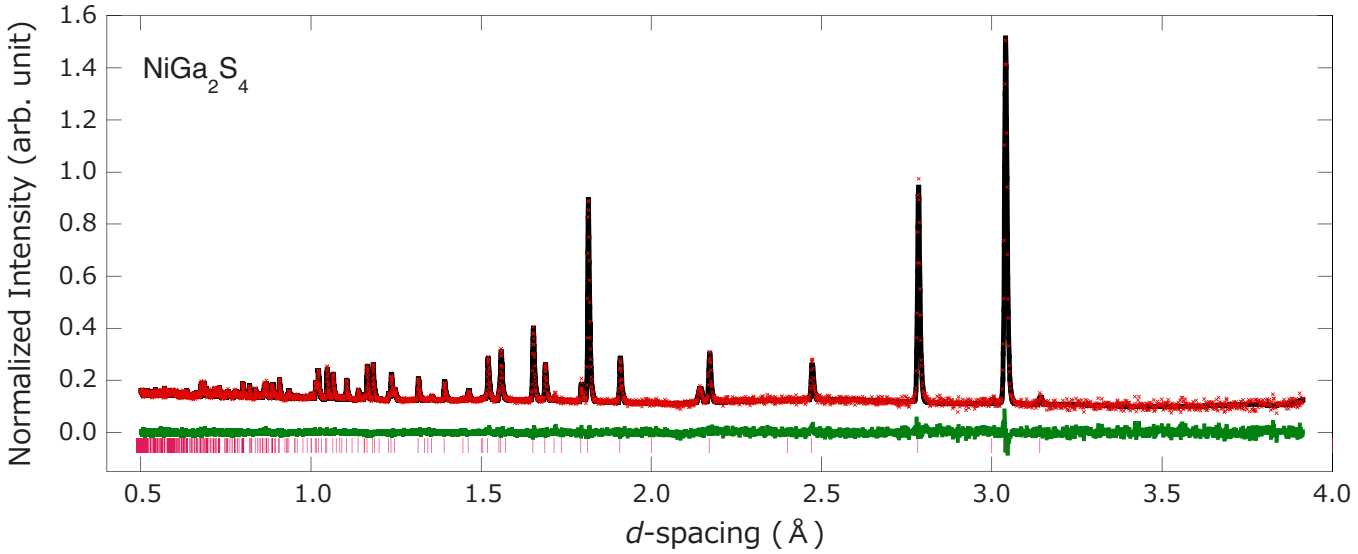

FIG. 1. (Color online) Final fit of the powder neutron-diffraction data collected for $NiGa_2S_4$ at room temperature. The green line represents the difference between the observed data (red crosses) and the calculated data (black solid line). The pink bars at the bottom show the positions of calculated (hkl) reflections.

are summarized in Table I, which are in good agreement with previous reports on the crystal structure.[2]

Occupancy fractions of Ni and Ga were refined in two analyses. Table I shows the refinement results when the occupancies of Ni and Ga were allowed to refine with no constraints. When the sum of Ni and Ga occupancies was fixed at unity, the $1b$ and $2d$ fractions both refined to respective values of 1.00(1). The lack of deviation from 1 for Ni and Ga fractions indicating $1b$ and $2d$ sites are only occupied by Ni and Ga, respectively, and that there is no site mixing between the two sites. This is consistent with the site preference of a Ni^{2+} ion for an octahedral site over a tetrahedral site.[20] Simultaneous refinements of isotropic displacement factors U_{iso} and occupancy fractions were stable, as indicated by the zero shift in estimated standard deviations and reduced χ^2 value of 1.220. Each of the refined values of U_{iso}, the measure of atomic motion about the equilibrium position at finite temperatures, is reasonably small and similar to each other, suggesting that occupancy fractions and atomic positions were refined properly. The low R_{wp} value and background assure that the two-dimensional triangular lattice in $NiGa_2S_4$ is only formed by Ni.

TABLE I. Crystallographic data, atomic coordinates, and isotropic displacement parameters for $NiGa_2S_4$ at room temperature.

Space group			$P\bar{3}m1$	
$a=b$(Å)			3.62676(3)	
c(Å)			12.0018(4)	
$\alpha=\beta$(°)			90	
γ(°)			120	
Cell volume (Å^3)			136.715(4)	
Temperature (K)			298	
No. of observations			5147	
No. of variables			41	
R_{wp} [a]			3.69%	
χ^2			1.220	
Atom	Wyckoff sites	z[b]	Occupancy fraction	U_{iso} (Å^3)
Ni	$1b$	$\frac{1}{2}$	1.005(6)	0.0094(8)
Ga	$2d$	0.2156(3)	0.995(6)	0.0076(8)
S1	$2d$	0.8687(5)	1.03(2)	0.0082(14)
S2	$2d$	0.4002(6)	0.98(2)	0.0054(13)

[a] $R_{wp}=\sqrt{\frac{\Sigma_i w_i(y_i^{obs}-y_i^{calc})^2}{\Sigma_i w_i(y_i^{obs})^2}}$.

[b] Atomic coordinates of $1b$ and $2d$ sites are (0, 0, $\frac{1}{2}$) and ($\frac{1}{3}$, $\frac{2}{3}$, z), respectively.

Figures 2(a) and 2(b) give the temperature dependence of the magnetic susceptibility $\chi \equiv M/H$ under $\mu_0 H=0.01$ and 7 T for typical concentrations of sulfur. All the compounds exhibit spin freezing under $\mu_0 H=0.01$ T as evident from the bifurcation between field-cooled (FC) and zero-field-cooled (ZFC) results. The spin freezing temperature T_f is determined to be the bifurcation temperature under 0.01 T. However, the bifurcation disappears under 7 T for all the samples with different nominal sulfur contents.

This enhancement in χ under 0.01 T compared to 7 T has been also observed in $Ni_{1-x}A_xGa_2S_4$. In these impurity substituted systems, the enhancement is found to originate not from the decoupled spins induced by impurities but mainly from the bulk spins because of the following experimental results.[10] (i) In A=Fe and Zn case of $Ni_{1-x}A_xGa_2S_4$, the freezing temperature T_f systematically changes from the one for pure $NiGa_2S_4$, being proportional to the Weiss temperature (θ_W). (ii) The low-temperature specific heat of $Ni_{1-x}A_xGa_2S_4$ including pure $NiGa_2S_4$ does not exhibit a notable field dependence, indicating the absence of the decoupled spins and their field polarization. In the current case of $NiGa_2S_{4+\delta}$, T_f is also found to be proportional to θ_W, namely, $T_f \sim 1/9 \times \theta_W$ [the inset of Fig. 2(d)], corresponding to the above experimental observation (i). This suggests that both

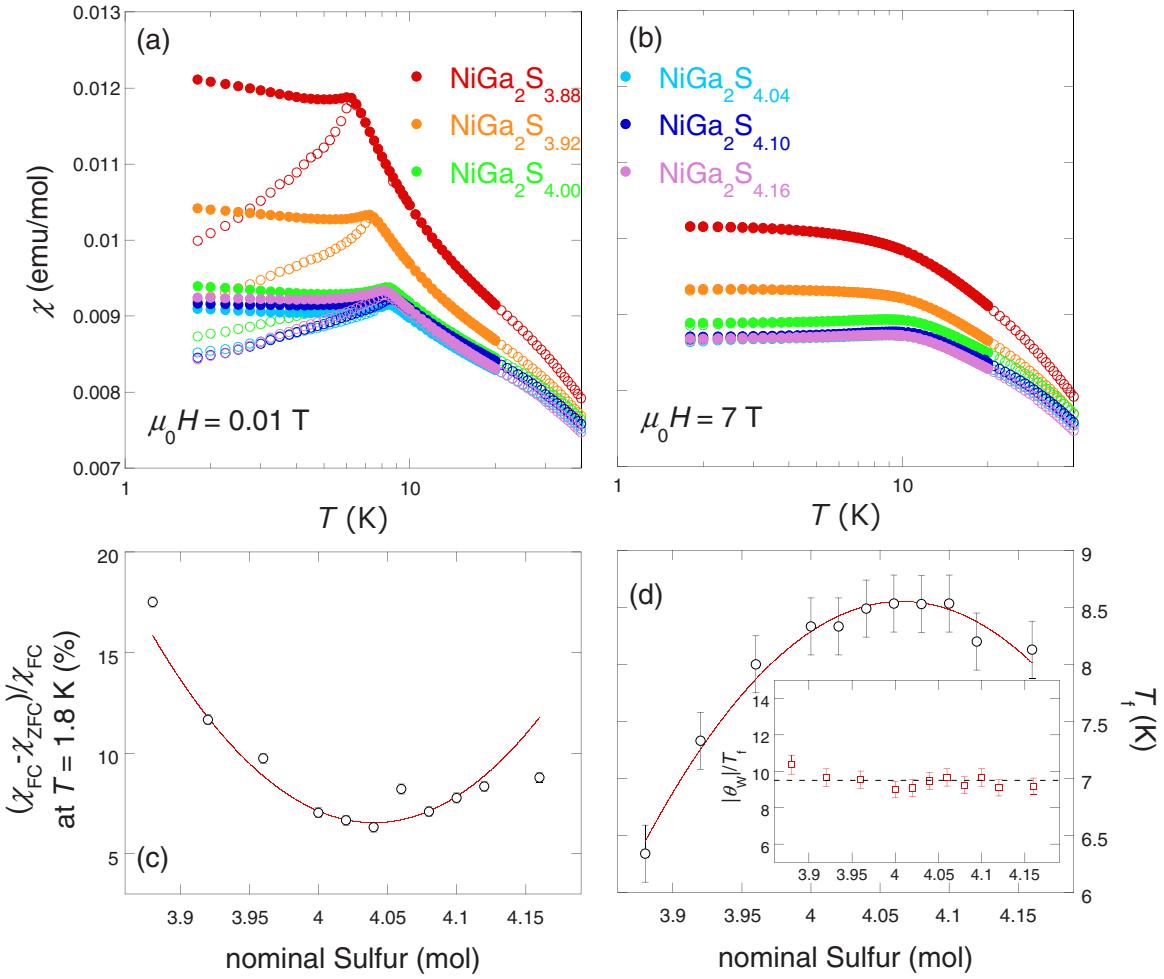

FIG. 2. (Color online) Temperature dependence of the magnetic susceptibility $\chi(T)$ under (a) $\mu_0 H = 0.01$ T and (b) 7 T for polycrystalline samples with typical concentration of sulfur. These are the data for both ZFC (open symbols) and FC (solid symbols) sequences. (c) Ratio $[(\chi_{FC}-\chi_{ZFC})/\chi_{FC}]$ between the size of the bifurcation $(\chi_{FC}-\chi_{ZFC})$ at $T=1.8$ K and the FC susceptibility (χ_{FC}) and (d) freezing temperature T_f against nominal sulfur contents. The solid lines are guides for the eyes. The inset shows the frustration parameter $(|\theta_W|/T_f)$ as a function of the nominal sulfur content.

T_f and the bifurcation of $\chi(T)$ are associated with bulk spin freezing.

Figures 2(c) and 2(d) give the ratio between the size of bifurcation $(\chi_{FC}-\chi_{ZFC})$ and FC susceptibility (χ_{FC}) at $T=1.8$ K, and T_f as a function of the nominal sulfur content, respectively. Our previous studies on the magnetic and nonmagnetic impurity effects on $NiGa_2S_4$ in the systems of $Ni_{1-x}A_xGa_2S_4$ with A=Mn, Co, and Zn have clarified that with increasing the impurity content $(\chi_{FC}-\chi_{ZFC})/\chi_{FC}$ apparently increases, while the freezing temperature T_f decreases as a function of the impurity concentration.[9,10] Notably, our results in Figs. 2(c) and 2(d) indicate that there appears a minimum of $(\chi_{FC}-\chi_{ZFC})/\chi_{FC}$ and a maximum of T_f at around nominal sulfur content of ~4.04. This suggests that the sample with the nominal sulfur content of ~4.04 is the most impurity/defect free and thus close to the stoichiometric concentration of sulfur. Previous inductively coupled plasma analysis for nominal $NiGa_2S_{4.00}$ reveals its actual composition as $Ni_{0.94(9)}Ga_{2.0(2)}S_{3.95(1)}$,[21] indicating that Ni and Ga are stoichiometric within error bars and resulting sulfur deficiency is about 1%. The actual amounts of sulfur in nominal $NiGa_2S_{4.00}$ and $NiGa_2S_{4.04}$ were determined by SEM-EDX measurements. The observed intensity as a function of energy was fitted, and the ratio of the molar amounts was decided under the constraint that the total amount of Ni, Ga, and S is normalized to 7. The results show that the averaged molar amounts of sulfur are 3.96(2) for nominal $NiGa_2S_{4.00}$ and 3.99(5) for $NiGa_2S_{4.04}$, respectively. The sulfur content of the nominal $NiGa_2S_{4.04}$ sample should most likely be stoichiometric.

On the basis of the above analyses, $NiGa_2S_{4.04}$ represents the most defect/impurity free stoichiometric samples among the obtained samples with different sulfur concentrations. Ga-NQR measurements have been performed for polycrystalline samples of $NiGa_2S_{4.00}$ and $NiGa_2S_{4.04}$ (see Fig. 3). As shown in Fig. 3, two intense peaks with narrow width [Ga(1)] and two weak peaks with broad width [Ga(2)] were observed both in $NiGa_2S_{4.00}$ and $NiGa_2S_{4.04}$. The frequency ratio of two intense peaks (16.5 MHz/10 MHz) is nearly the same as that of two weak peaks (12.5 MHz/7.5 MHz), which is equal to the ratio of the nuclear quadrupole moment $(^{69}Q/^{71}Q=1.589)$. This indicates that there are two sets of

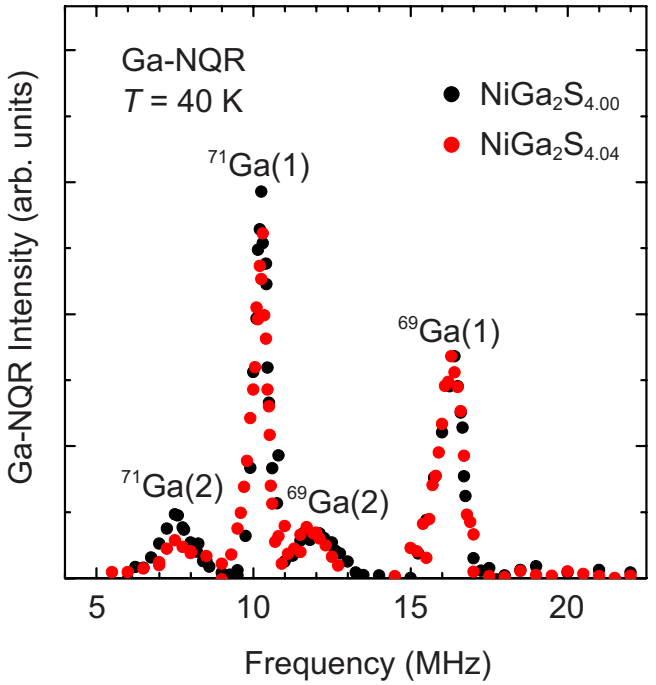

FIG. 3. (Color online) ^{69,71}Ga-NQR spectra for polycrystalline $NiGa_2S_{4.00}$ and $NiGa_2S_{4.04}$ at $T=40$ K.

distinct NQR signals and reveals the existence of two Ga sites with different EFGs in $NiGa_2S_4$. The Ga-NQR spectrum in $NiGa_2S_{4.04}$ is almost identical to that of $NiGa_2S_{4.00}$; the peak intensities of the two Ga sites in the $NiGa_2S_{4.04}$ spectrum have the same ratio as peak intensities in $NiGa_2S_{4.00}$. If the different EFG was caused by sulfur deficiency or excess, the intensities of the Ga(2) signals in $NiGa_2S_{4.04}$ should be different from those in $NiGa_2S_{4.00}$. However, as shown in Fig. 4, the identical spectra for both compounds strongly suggest that two Ga sites are neither due to sulfur deficiency nor extra inclusion. Alternatively, we consider that an inclusion of different stacking units closely related to the structure of $NiGa_2S_4$ might give rise to an additional Ga site with a different EFG. In order to check such a possibility in the crystal structure, TEM investigations were employed.

Single crystals with the nominal content $NiGa_2S_{4.04}$ were used for the TEM studies. Figures 4(a) and 4(b) show a TEM image and a diffraction pattern for the *ab* plane, respectively. The TEM image in Fig. 4(a) indicates no sulfur deficiency

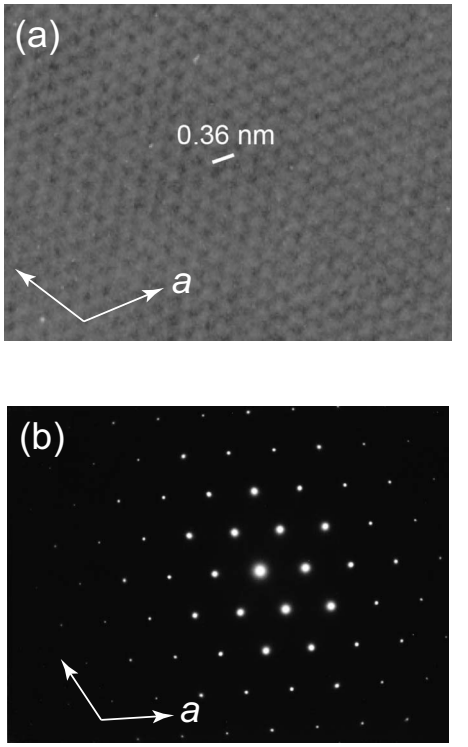

FIG. 4. (a) High-resolution transmission electron microscopy images of the NiS_2 layer in the $NiGa_2S_{4.04}$ single crystal. (b) Electron-diffraction patterns along the *ab* plane. They were taken at room temperature.

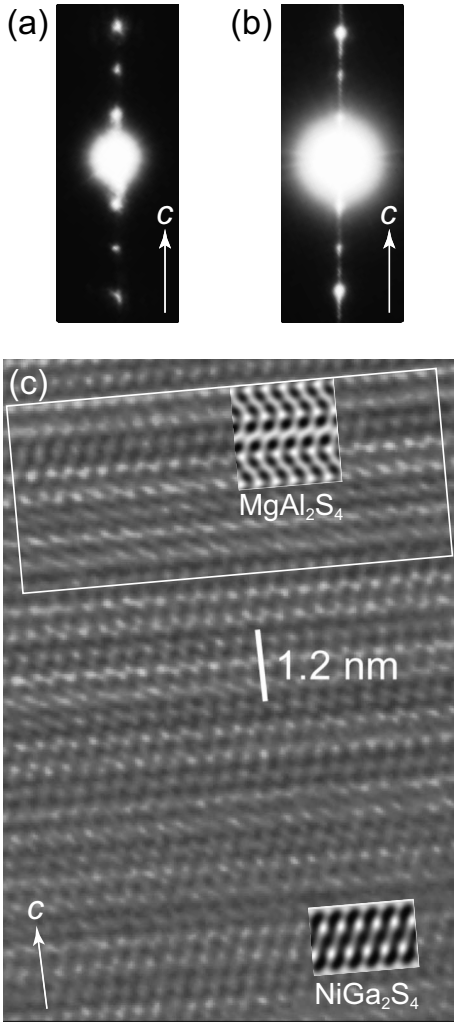

FIG. 5. Electron diffraction patterns along the *c* axis (a) without split spots and (b) with split spots for the $NiGa_2S_{4.04}$ single crystal. (c) High-resolution transmission electron microscopy images projected along the direction parallel to the *c* axis with the simulated images for $NiGa_2S_4$ (Ref. 2) and $MgAl_2S_4$ (Ref. 23) obtained using the MACTEMPAS software. They were taken at room temperature. The region for the one layer unit surrounded by a white rectangle shows a texture clearly different from the other main matrix layer sequence.

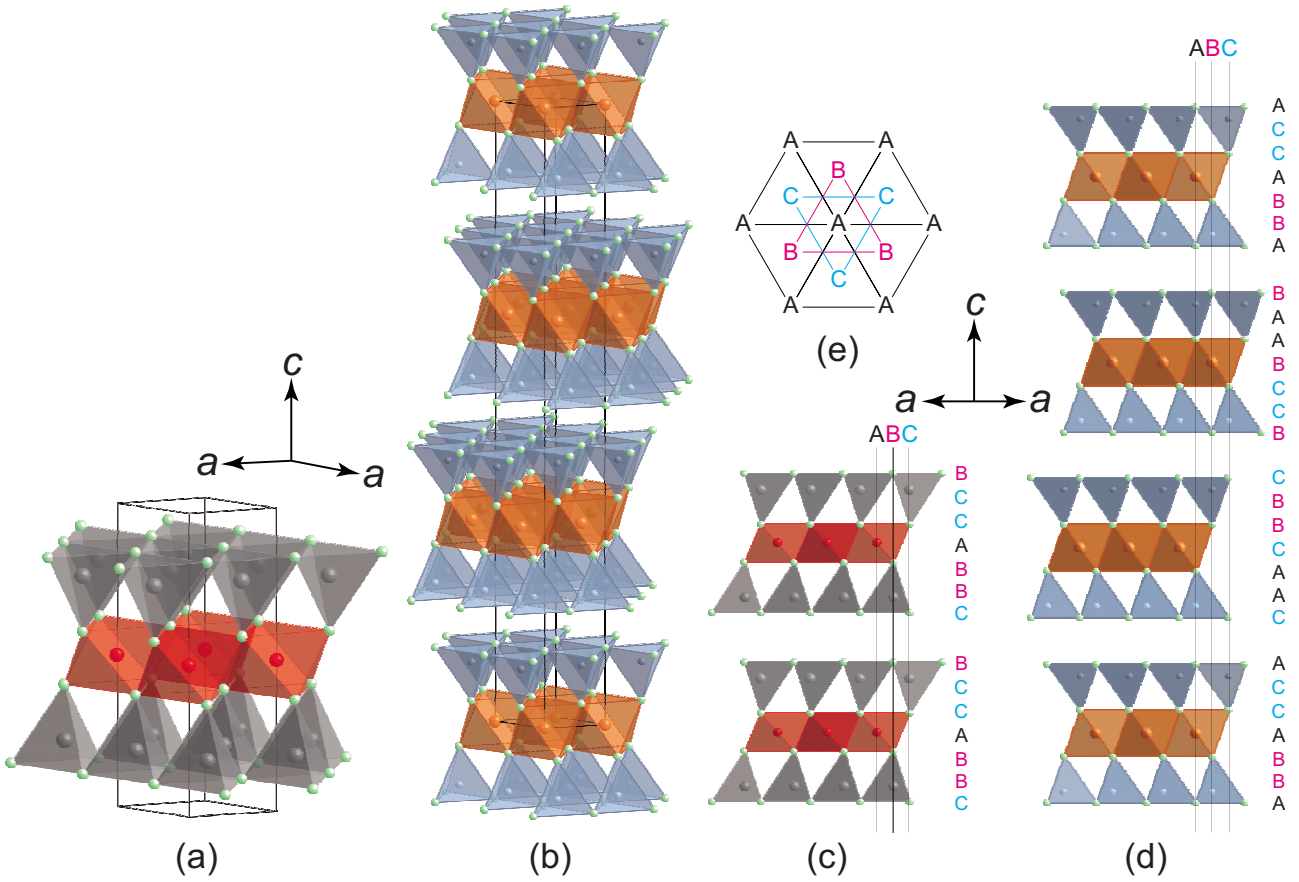

FIG. 6. (Color online) Crystal structures of (a) $NiGa_2S_4$ ($Z=1$) with space group $P\bar{3}m1$ (Ref. 2) and (b) $MgAl_2S_4$ ($Z=3$) with space group $R\bar{3}mH$ (Ref. 23). The stacking sequences of hexagonal closest packing for each atom in (c) $NiGa_2S_4$ and (d) $MgAl_2S_4$ are presented using the definition of the position given in the inset (e).

within the resolution of the instrument. Furthermore, clean electron-diffraction patterns were obtained for all the images taken for the *ab* plane, as shown in Fig. 4(b), which is consistent with the trigonal crystal structure obtained by the neutron-diffraction analyses. This indicates that the compound has a nearly perfect NiS_2 triangular lattice layers with no distortion.

We have also performed the TEM observations along the *c* axis. Similar to the case for the *ab* plane, diffraction patterns along the *c* axis for most parts of the crystals were found to be well defined and consistent with the crystal structure obtained by neutron-diffraction analyses [Fig. 5(a)]. However, a few diffraction peaks along the *c* axis are found to split, as shown in Fig. 5(b). The origin of split spots may be due to the coexistence of different stacking sequences. The actual displacement between the diffraction spots r_{hkl} in the photograph of diffraction patterns are represented as

$$d_{hkl}r_{hkl} = L\lambda, \tag{1}$$

where d_{hkl} is the surface spacing in the crystal, L is the camera length (100 cm), and λ is the wavelength of electron beam (2.51 pm). In the case of a trigonal crystal structure, d_{hkl} is given by

$$\frac{1}{d_{hkl}^2} = \frac{4}{3a^2}(h^2 + hk + k^2) + \frac{1}{c^2}l^2, \tag{2}$$

with using the lattice constants a and c, and Miller indices h, k, and l. Therefore, the split spots, which correspond to a shorter r_{hkl} than the one expected for $NiGa_2S_4$ with $Z=1$ in Ref. 2, suggest the coexistence of different stacking sequences, for example, generating $Z>1$. This kind of split spots due to a stacking fault is reported for several layered materials such as (In, Ga)N alloys.[22] On the other hand, the compound closely related to $NiGa_2S_4$ and $MgAl_2S_4$ (Ref. 23) consists of MgS_6 octahedra and AlS_4 tetrahedra. This compound, however, has a lattice constant c three times longer than that of $NiGa_2S_4$ (Fig. 6), and as a result, three Mg^{2+} cations in the unit cell of $MgAl_2S_4$, leading to $Z=3$.

This difference in Z or the unit-cell size actually comes from the difference in the stacking sequence. In $NiGa_2S_4$ and $MgAl_2S_4$, all the atoms form an exact triangular lattice but, as shown in Figs. 6(c) and 6(d), there is a distinction in the stacking sequence even in one layer. In Fig. 6, each index in a layer corresponds to the outer S Ga (Al), inner S Ni (Mg), inner S Ga (Al), and outer S from the top to the bottom. In $NiGa_2S_4$, when Ni takes the position of A, the outer S should be located at the position of B or C. On the other hand, in $MgAl_2S_4$ structure, reflecting $Z=3$, Mg can take three posi-

tions within the unit cell and the outer S invariably takes the same position as Mg. This variety of stacking sequences within one layer may well produce the different EFGs at the Ga sites.

In order to confirm such a possible stacking fault, we have taken images along the *c* axis carefully and found a few images with a stacking fault, as shown in Fig. 5(c). The region for the one layer unit surrounded by a white rectangle in Fig. 5(c) shows a texture clearly different from the other main matrix layer sequence. In order to further check the origin of the stacking fault, we made the simulations of the diffraction patterns using the multislice method of MACTEMPAS software.[19] In Fig. 5(c), the simulation results for $NiGa_2S_4$ and $MgAl_2S_4$ were shown on top of the optical TEM image. The result suggests that the stacking fault in the image may be due to the inclusion of structures with the $MgAl_2S_4$ ($Z=3$) type of stacking. Such an inclusion of different stacking units may give rise to an additional Ga site with a different EFG. In addition, the amount of the stacking fault should not be affected by a tiny sulfur deficiency. It is important to search for a synthesis method to further diminish the amount of different Ga sites, for example, by changing the annealing temperature.

IV. CONCLUSIONS

We have succeeded in synthesizing polycrystalline samples of $NiGa_2S_{4+\delta}$ with nominal contents ranging between $-0.12 \leq \delta \leq +0.16$ and also succeeded in growing single crystals of $NiGa_2S_{4.04}$. They maintain the same trigonal structure with the space group $P\bar{3}m1$. Time-of-flight neutron-diffraction measurements have confirmed the triangular lattice structure and the absence of site mixing between Ni and Ga. Furthermore, magnetic-susceptibility results and chemical analyses indicate that the sample with the nominal concentration of $NiGa_2S_{4.04}$ should be stoichiometric without sulfur deficiency. On the other hand, "Ga two sites" have been observed by the NQR measurements even for $NiGa_2S_{4.04}$, pointing to other possibilities of structural defects besides a sulfur deficiency. The TEM observations along the *ab* plane have shown the existence of a clean defect-free NiS_2 triangular lattice plane, while a few cases of the observations along the *c* axis indicate split spots due to stacking faults. Further comparison with simulated images confirms the existence of a stacking fault, which may well be the origin of the two sites of Ga observed in the NQR spectra.

ACKNOWLEDGMENTS

The authors are grateful to Masaki Ichihara for his invaluable support in TEM observations at the Institute for Solid State Physics, the University of Tokyo. We acknowledge Z. Hiroi and Y. Maeno for discussion. This work is partially supported by a Grant-in-Aid under Grant No. 18684020 from the Japanese Society for the Promotion of Science and also by Grant-in-Aid for Scientific Research on Priority Areas under Grant Nos. 17071003, 19052003 from the Ministry of Education, Culture, Sports, Science and Technology, Japan. Y.N. acknowledges support from the Japan Society for the Promotion of Science for Young Scientists.

[1] A. P. Ramirez, in *Handbook of Magnetic Materials*, edited by K. H. J. Buschow (Elsevier, Amsterdam, 2001), Vol. 13, pp. 423–520.
[2] H. D. Lutz, W. B. Buchmeier, and H. Siwert, Z. Anorg. Allg. Chem. **533**, 118 (1986).
[3] S. Nakatsuji, Y. Nambu, H. Tonomura, O. Sakai, S. Jonas, C. Broholm, H. Tsunetsugu, Y. Qiu, and Y. Maeno, Science **309**, 1697 (2005).
[4] H. Takeya, K. Ishida, K. Kitagawa, Y. Ihara, K. Onuma, Y. Maeno, Y. Nambu, S. Nakatsuji, D. E. MacLaughlin, A. Koda, and R. Kadono, Phys. Rev. B **77**, 054429 (2008).
[5] D. E. MacLaughlin, Y. Nambu, S. Nakatsuji, R. H. Heffner, Lei Shu, O. O. Bernal, and K. Ishida, Phys. Rev. B **78**, 220403(R) (2008).
[6] C. Stock, S. Jonas, C. Broholm, S. Nakatsuji, Y. Nambu, K. Onuma, Y. Maeno, and J.-H. Chung (unpublished).
[7] Y. Nambu, M. Ichihara, Y. Kiuchi, S. Nakatsuji, and Y. Maeno, J. Cryst. Growth **310**, 1881 (2008).
[8] S. Nakatsuji, H. Tonomura, K. Onuma, Y. Nambu, O. Sakai, Y. Maeno, R. T. Macaluso, and J. Y. Chan, Phys. Rev. Lett. **99**, 157203 (2007).
[9] Y. Nambu, S. Nakatsuji, and Y. Maeno, J. Phys. Soc. Jpn. **75**, 043711 (2006).
[10] Y. Nambu, S. Nakatsuji, Y. Maeno, E. K. Okudzeto, and J. Y. Chan, Phys. Rev. Lett. **101**, 207204 (2008).
[11] F. Gautier, G. Krill, M. F. Lapierre, and C. Robert, J. Phys. C **6**, L320 (1973).
[12] F. G. Donika, S. I. Radautsan, S. A. Semiletov, T. V. Donika, I. G. Mustya, and V. F. Zhitar', Sov. Phys. Crystallogr. **15**, 695 (1971).
[13] F. G. Donika, S. I. Radautsan, G. A. Kiosse, S. A. Semiletov, T. V. Donika, and I. G. Mustya, Sov. Phys. Crystallogr. **16**, 190 (1971).
[14] F. G. Donika, S. I. Radautsan, S. A. Semiletov, G. A. Kiosse, and I. G. Mustya, Sov. Phys. Crystallogr. **17**, 575 (1972).
[15] F. Lappe, A. Niggli, R. Nitsche, and J. G. White, Z. Kristallogr. **117**, 146 (1962).
[16] J. D. Jorgensen, J. Faber, Jr., J. M. Carpenter, R. K. Crawford, J. R. Haumann, R. L. Hitterman, R. Kleb, G. E. Ostrowski, F. J. Rotella, and T. G. Worlton, J. Appl. Crystallogr. **22**, 321 (1989).
[17] A. C. Larson and R. B. Von Dreele, Los Alamos National Laboratory Report No. LAUR 86, 2000 (unpublished).
[18] B. H. Toby, J. Appl. Crystallogr. **34**, 210 (2001).
[19] MACTEMPAS, total resolution (www.totalresolution.com).
[20] S. Viticoli, Prog. Cryst. Growth Charact. **13**, 105 (1986).
[21] S. Jonas and C. Broholm (private communication).
[22] H. K. Cho, J. Y. Lee, K. S. Kim, and G. M. Yang, Appl. Phys. Lett. **77**, 247 (2000).
[23] H. Haeuseler and S. K. Srivastava, Z. Kristallogr. **215**, 205 (2000).